

This is an Open Access document downloaded from ORCA, Cardiff University's institutional repository: <https://orca.cardiff.ac.uk/id/eprint/172434/>

This is the author's version of a work that was submitted to / accepted for publication.

Citation for final published version:

Li, Yating, Li, Yongjian, Lin, Zhiwei, Yue, Shuaichao, Chen, Ruiying, Guo, Peng and Liu, Jun 2024. A hysteresis model for soft magnetic composites considering particle size distribution. IEEE Transactions on Magnetics 60 (12) , 7301405. 10.1109/TMAG.2024.3458798

Publishers page: <http://dx.doi.org/10.1109/TMAG.2024.3458798>

Please note:

Changes made as a result of publishing processes such as copy-editing, formatting and page numbers may not be reflected in this version. For the definitive version of this publication, please refer to the published source. You are advised to consult the publisher's version if you wish to cite this paper.

This version is being made available in accordance with publisher policies. See <http://orca.cf.ac.uk/policies.html> for usage policies. Copyright and moral rights for publications made available in ORCA are retained by the copyright holders.



A Hysteresis Model for Soft Magnetic Composites Considering Particle Size Distribution

Yating Li¹, Yongjian Li^{1*}, Zhiwei Lin^{1,3}, Shuaichao Yue¹, Ruiying Chen¹, Peng Guo¹, Jun Liu²

¹ State Key Laboratory of EERI, Hebei University of Technology, 300130, Tianjin, China

² School of Engineering, Cardiff University, Cardiff CF24 3AA, U.K

³ Ningbo Magnetic Materials Application Technology Innovation Center Co., Ltd, 315201, Ningbo, China

This paper presents a hysteresis model that incorporates the microstructural features of soft magnetic composites (SMCs). The anhysteresis curve is derived based on Globus's model, which characterizes the continuous displacement of the domain wall within the particles. A static hysteresis model is then formulated by incorporating the particle size-related pinning field in the Energy-Based model to describe irreversible displacement. An inverse dynamic model is further developed considering the relation between the eddy current effect and particle size. The model accuracy is validated by comparing the calculated hysteresis loops and iron loss of two types of SMCs samples with experimental results under both quasi-static and dynamic conditions.

Index Terms—Hysteresis model, Iron loss, Particle size distribution, Soft magnetic composites

I. INTRODUCTION

SOFT magnetic composites are made of iron powders with insulation coating. They are widely used in three-dimensional magnetic flux machines due to their excellent magnetic and thermal isotropy [1]. Meanwhile, SMCs exhibit superior characteristics for application in high-frequency excitations due to their lower eddy current and high electrical resistivity. It is well known that the properties of SMCs are determined by microstructural features such as particle size distribution, dislocation, and doping rate [2]. Thus, it is necessary to correlate the magnetic property with the microstructural features of the material to develop hysteresis models with high accuracy and extensibility.

There have been several methods for modelling the hysteresis property of ferromagnetic materials. The classic Preisach model and its extended versions feature high accuracy and mathematical robustness but lack physical meaning. There has been a preliminary attempt of linking the threshold of hysterons, i.e., local elementary coercivity phenomenologically to the pinning strength of associated microstructural features to domain walls [3]. However, the parameter identification is complex and the identification process is still being optimized [4]. The Jiles-Atherton (J-A) model is a popular physical model based on the domain theory [5] but performs poorly in minor loop modelling. An effective approach to simply implement the model and accurately characterize minor loops is to decompose the applied field into an irreversible and reversible field. Since the separated magnetic field components correspond to domain wall irreversible motion and reversible motion, the microstructural features can be inherently incorporated. The Energy-Based (EB) model leverages the advantages of both the J-A model and the Preisach model [6] and looks at magnetic hysteresis from the energy point of view. Its hysteron represents the pinning process as a friction-like force to calculate the irreversible and reversible fields. The magnetization is calculated by summing hysterons of different sizes, enabling the model to predict the minor hysteresis loops considering

microstructural features as pinning sites.

The existing EB model does not take microstructure into account. The microstructures, e.g., the iron particle size, of SMCs significantly affect the domain structures, which in turn influences the magnetization process and magnetic properties [7]. This paper proposes an EB hysteresis model for SMCs considering their particle size distribution using the Globus approach. Globus proposed a treatment for domain boundary motion, introducing the concept of domain wall size, grain size, and the physical representation of reversible and irreversible domain wall motion processes efficiently [8]. Besides the hysteresis loss caused by irreversible movement of the domain wall, sudden jumps also generate the eddy current, causing dynamic dissipation. In heterogeneous materials like SMCs, the eddy current producing region is refined according to the particles [9]. The proposed model will also incorporate particle size-dependent eddy currents.

In this paper, we explain how particle size distribution has been incorporated into a hysteresis model by characterizing the domain wall motion. The model establishes a quantitative connection between microstructural features of interest and magnetic properties. The rest of this paper is organized as follows. In Section II, the reversible and irreversible domain wall motion within a single particle and multi particles are formulated based on Globus's assumption and EB model. Then the inverse dynamic model is developed. In Section III, the experimental system and parameters identification are presented. And the proposed model is verified by comparing with the experimental measurements.

II. THEORY

A. The Static Magnetization within a Single Particle

Consider the domain processes in a single particle during magnetization, when the applied external magnetic field changes, the domain structure will change to minimize the total energy of the system. The relationship between Bloch domain wall movement and energy changes needs to be established. According to Globus's assumption, the particle is represented as sphere with a diameter of D , divided into antiparallel magnetic domains by a Bloch domain wall, as shown in Fig. 1.

This work was supported in part by the National Natural Science Foundation of China under Grant 52130710, 52407005, in part by the Funds for Creative Research Groups of Hebei Province (No. E2024202298), and in part by the Cultivate Foundation of Innovation Ability of Hebei Education Department for Ph.D. Student under Grant CXZZBS2024034.

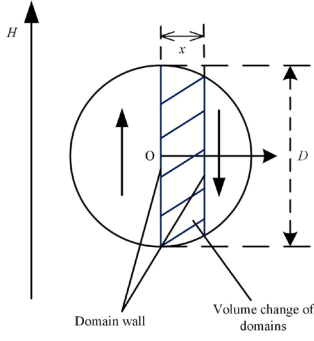


Fig. 1. Displacement x of the Bloch domain wall in a single particle.

The state of the domain wall can be analytically solved by the change of energy. The change of Zeeman energy ΔE_z is expressed as [8]

$$\Delta E_z = -2\mu_0 M_s H \Delta V = -2\mu_0 M_s H (r^2 x - \frac{1}{3} x^3) \pi, \quad (1)$$

where ΔV is the change of volume, M_s the saturation magnetization, $r = D/2$ the radius of the particle, and x the displacement of the domain wall. The driving force F_m for the domain wall movement can be obtained from

$$F_m = -\frac{d\Delta E_z}{dx} = 2\mu_0 M_s H (r^2 - x^2) \pi. \quad (2)$$

The area of the domain wall decreases during the wall motion process. The resistance, F_γ due to the change of domain wall energy, is assumed to vary with the area of the domain wall. The F_γ is expressed as

$$F_\gamma = \gamma \frac{dA}{dx} = \gamma 2\pi x, \quad (3)$$

where γ is the wall energy per unit area, and A the surface area of the wall expressed as $\pi(r^2 - x^2)$. In the equilibrium state, F_m is equal to F_γ , then it could be deduced to

$$2\mu_0 M_s H (r^2 - x^2) \pi = 2\pi \gamma x. \quad (4)$$

The magnetization M is proportional to the change of volume ΔV in a spherical particle with volume V . Thus, the magnetization is expressed as

$$M = 2M_s \frac{\Delta V}{V} = 2M_s \frac{r^2 x - \frac{1}{3} x^3}{\frac{4}{3} \pi r^3} = M_s (3\xi - 4\xi^3), \quad (5)$$

where ξ is x/D . Domain walls are assumed to be rigid at first approximation. That is, the bending of the domain wall is neglected.

The irreversible domain wall motion is strongly influenced by pinning sites created by technological processes. This pinning force is analogous to friction, which opposes the wall motion and causes magnetic hysteresis. After figuring out the phenomenological treatment of the pinning effect, that is, friction force, we opt for the EB model with dry-friction-like hysterons to describe the hysteresis characteristic of the magnetic material. The domain wall jumps to the next pinning site when the change in energy is sufficient to overcome the pinning field H_{pin} . Otherwise, the domain wall remains pinned. The magnetization is calculated by the updated reversible field $H_r(t)$ [6], expressed as

$$H_r(t) = \begin{cases} H(t) - H_{pin} & \text{if } |H(t) - H_r(t-1)| \geq H_{pin} \\ H_r(t-1) & \text{otherwise} \end{cases}, \quad (6)$$

where $H_r(t-1)$ is the calculated result at the previous step.

The pinning field H_{pin} depends on the particle size [7]. The SMC sample made with large particles has fewer gaps and hence a weaker demagnetizing field. However, small particles lead to a stronger demagnetizing field and more defects due to the increased particle surface. As a result, the relationship between the pinning field and the particle size is phenomenologically established as follows

$$H_{pin}(\alpha) = p_1 / \alpha^{p_2}, \quad (7)$$

where α is the ratio of diameter D of particle to the average diameter of particle D_{avg} and p_1 and p_2 are fitted parameters that are independent of particle size.

The combination of the EB model and the Globus model characterizes both reversible and irreversible domain wall motion. The state of the domain wall in each particle can be determined. At a certain stable magnetic field, when the applied magnetic field H is equal to or less than the pinning field H_{pin} , the domain structure remains stable. By continuously increasing the field, the wall starts to move towards the boundary of the particle. The maximum displacement of the domain wall ξ_{max} is about half of the diameter if the applied field is high enough to saturate the sample. Meanwhile, the length (or area) of the domain wall decreases and ultimately vanishes when the wall reaches the surface of the spherical particle. Conversely, if the magnetic field H is decreased gradually after saturation, a slightly decreasing magnetic field will not result in the domain wall moving backward due to the existence of the friction force until it overcomes the pinning field H_{pin} . γ which represents wall energy per unit area influences the slope of the anhysteresis curve. p_1 and p_2 , which represent the relation of coercivity between particle size, influence the width of the hysteresis loop.

B. The Magnetization of Multi Particles

The above-mentioned analysis is based on a single spherical particle. However, the real SMCs consist of particles with a variety of sizes. Magnetic properties are highly correlated with the distribution of particle sizes. Consider particles with a Gaussian size distribution in the range between $0.1D_{avg}$ and $2D_{avg}$, i.e., $\alpha_k = [0.1, 2]$ being magnetized. The particles whose sizes are outside this range are ignored due to their low probability. The displacement of the domain wall in the particle k with size α_k is calculated (4) with H_r^k , the reversible field of the particle k . The pinning field H_{pin}^k of the particle k is calculated by (7) with α_k . The magnetization in each particle m_k is calculated by (5). The total magnetization m_t is obtained by [10]

$$m_t = \sum_k m_k P(\alpha_k), \quad (8)$$

where $P(\alpha_k)$ is the proportion of particles with size α_k in the sample, which is calculated by the probability density function P_p of the samples, expressed as

$$P(\alpha_k) = \int_{\alpha_k}^{\alpha_{k+1}} P_p(\alpha) d\alpha, \quad (9)$$

where

$$P_p(\alpha) = \sum_{i=1}^{N_1} \omega_i e^{-\left(\frac{\alpha - \mu_i}{\sigma_i}\right)^2}. \quad (10)$$

N_1 , ω_i , μ_i and σ_i are parameters fitted by the microfeature data provided by the manufacturer. The sum of $P(\alpha_k)$ equals 1.

When particles of different sizes are magnetized, the domain processes are different. Since the pinning field H_{pin} is inversely proportional to the particle size, the large-size particle has a low H_{pin} while the small-size particle has a high H_{pin} . Thus, domain wall motion in the large particles starts at a lower field, while in small particles it starts at a higher field. Consequently, as the magnetic field increases, large particles are magnetized and saturated earlier than small particles.

C. The Inverse Dynamic Model

Although the model with imposed magnetic field strength H_{static} conforms to the magnetization mechanisms. The inverse model under magnetic flux density $B(t)$ imposed conditions is more convenient to use in the finite element method [11]. The relationship between the H_{static} and the displacement of the domain wall x from (4) is expressed as

$$H_{static} = \frac{2\pi\gamma x}{2\mu_0 M_s (r^2 - x^2)\pi}. \quad (11)$$

It is assumed that the displacement of the domain wall is proportional to the input magnetic flux density $B(t)$ [12], expressed as

$$x(t) = cB(t)r, \quad (12)$$

where c is the proportion coefficient of the relation. The reversible magnetic flux density $B_r(t)$ is defined as

$$B_r(t) = \begin{cases} \text{if } |B(t) - B(t-1) + B_r(t-1)| \leq B_{pin} \\ B(t) - B(t-1) + B_r(t-1) \\ \text{otherwise} \\ B_{pin} \end{cases}, \quad (13)$$

where B_{pin} is also assumed to have a power-law dependence on the grain size with a negative exponent expressed as (7). The imposed $B(t)$ is used to calculate $B_r(t)$ by (13), and then the magnetic field strength is calculated by (11) with the domain wall displacement state calculated by (12).

However, the quasi-static model is insufficient to model hysteresis characteristics at higher frequencies. The dissipation caused by hysteresis is also related to the rate of domain wall motion. The sudden change in the position of the wall induces various magnetization, generating Joule dissipation caused by the eddy current. The eddy current dissipated in SMCs can be divided into two parts. One part flows in the interior of a well-insulated powder particle, and the other flows within the entire cross-section for a material in which the insulation is broken [1]. It is known that the insulating coating in SMCs barriers the inter-particle eddy current path at dynamic excitations. The flow of the eddy current is mainly within the particle. Thus, the total eddy current is determined by the particle size, electrical resistivity, and shape of the sample. Inspired by the [1,13], the equivalent magnetic field component caused by the eddy current, H_{ed} , is defined as

$$H_{ed} = p_3 \alpha^{p_4} \frac{dB(t)}{dt}, \quad (14)$$

where p_3 and p_4 are fitted parameters. The eddy current field H_{ed} describes the relationship between the particle size and eddy current dissipation, which increases with the increase of particle size. The dynamic model is separated into two components, that is the hysteresis component and the eddy current component, reducing complexity while maintaining accuracy [14].

III. VERIFICATION AND DISCUSSION

A. Experimental System and Parameters of the Sample

SOMALLOY™ 700HR5P800MPa and 130i5P800MPa ring samples are utilized to verify the presented model. The density of 700HR5P800MPa is 7.5 g/cm³, and 130i5P800MPa is 7.44 g/cm³. The primary turns of the samples are 240, and the secondary turns are 10. The thickness of the samples is 5 mm, and the outer/inter diameter is 55 mm/45 mm. The AMH-1M-S testing system is employed to measure the magnetic properties of the sample, utilizing the ring sample method, as shown in Fig.2. More details can be found in [15]. The magnetic characteristics of the samples under quasi-static excitation (10 Hz) and dynamic excitation are measured by the experimental system. The measured loops are shown in Fig. 3 with different magnetic flux density amplitude B_m . The average diameter D_{avg} of 700HR5P800MPa is about 300 μ m, while the diameter of the 130i5P800MPa is about 130 μ m.

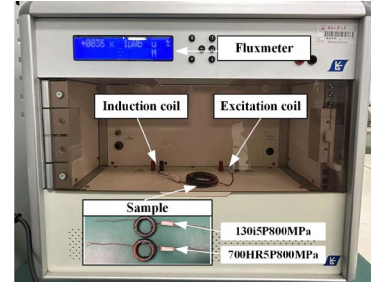


Fig.2 Measurement system and samples

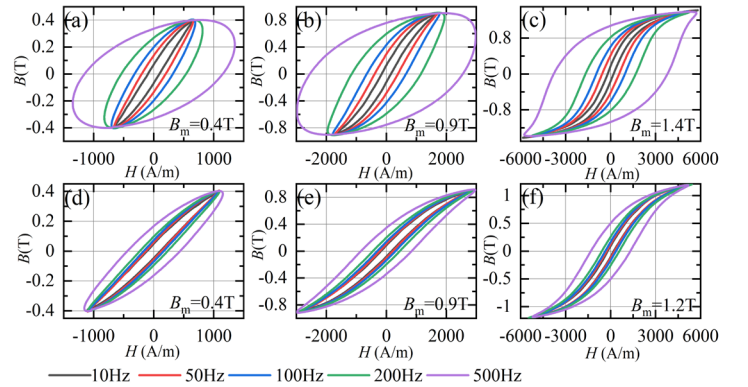


Fig.3 Measured hysteresis loops under quasi-static excitation and dynamic excitation for 700HR5P800MPa in (a), (b), (c) and 130i5P800MPa in (d), (e), (f).

B. Verification of Proposed Model

The data used for identification includes the hysteresis loops with different sizes under quasi-static and dynamic excitation measured in Section A. The parameters in the static model including γ , M_s , p_1 , and p_2 are identified by minimizing the least-squares residual over all measured quasi-static loops.

The trust-region-reflective algorithm is adapted. 100 particles with different sizes are assumed to be magnetized. Their pinning field is calculated by (7). The discrete probability density parameters of the original EB model are replaced by (10). The objective function for the identification procedures is defined as

$$\varepsilon_1 = \frac{1}{N} \sum_{i=1}^N |B_{m,i} - B_{c,i}|, \quad (15)$$

where N is the number of data, B_m and B_c are the measured and calculated magnetic flux density. Fig. 4 (a) shows the particle size distribution received from the manufacturer. The data align with the distribution function given in Eq. (10), where the parameters are obtained by fitting using Curve Fitting Toolbox of MATLAB, and the value of parameters are listed in (a). Fig. 4 (b) and (c) show the comparison between the calculated and measured loops. A good match over a wide range of magnetic flux densities is obtained. The iron loss W is calculated by the area of hysteresis loops. The comparison between the measured iron loss and calculated ones of different values of B_m is shown in Fig. 5. The average error is 5.18% for 700HR5P800MPa and 5.23% for 130i5P800MPa.

The magnetic hysteresis loops under dynamic excitations at 50 Hz, 100 Hz, 200 Hz, and 500 Hz are calculated by the proposed inverse dynamic hysteresis model. The objective function for identification is defined as

$$\varepsilon_2 = \frac{1}{N} \sum_{i=1}^N |H_{m,i} - H_{c,i}|, \quad (16)$$

where H_m and H_c are the measured and calculated magnetic field strength. c , γ , p_1 , and p_2 are identified by the loops with different sizes under quasi-static excitation, M_s is obtained from static model, and p_3 and p_4 are identified by the dynamic data. These parameters are suitable for a wide range of magnetic flux densities and frequencies. Fig. 6 shows the hysteresis loops under dynamic excitations and the comparison between the measured and calculated iron loss is shown in Fig. 7. Two types of SMC samples present different hysteresis loops and iron loss. 700HR5P800MPa with larger particles has wider loops and higher loss, while 130i5P800MPa with smaller particles has lower loss. Due to the insulating coating, the intra-particle eddy current dominates the total eddy current loss, rather than the inter-particle eddy current. Thus, the sample made from the iron particles with a smaller size shows less loss than that made from the larger size. The average error values obtained over all frequencies and magnitudes of 700HR5P800MPa and 130i5P800MPa are 6.78% and 10.42%, respectively. The error is mainly caused by the difference between the calculated and measured coercive field. The coercive field is expressed by the sum of the pinning field of particles with different sizes. The sample with larger particles contains fewer gaps, resulting in lower demagnetization. However, the sample with smaller particles contains more non-magnetic regions, which are not accounted in the model. Thus, the difference between the calculated and measured loss for 130i5P800MPa is higher than for 700HR5P800MPa. It can be seen that the proposed model could calculate the hysteresis loops and iron loss of

SMCs with different particle size distributions accurately.

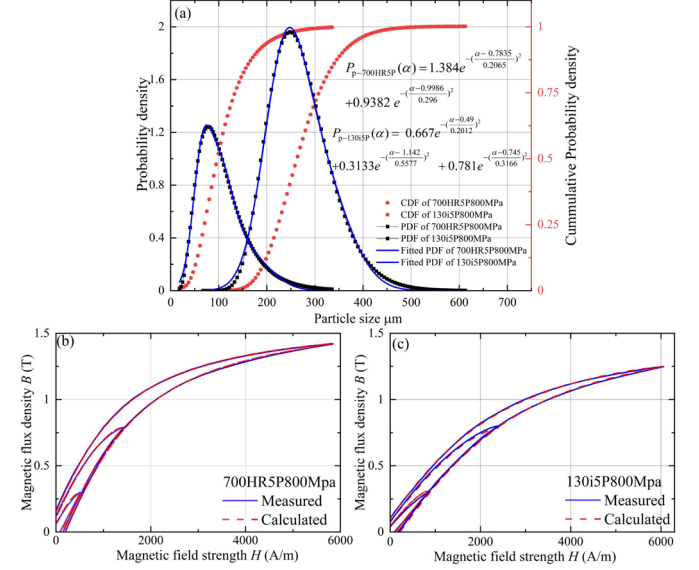


Fig. 4. Measured and calculated hysteresis loops at 10 Hz using particle size distribution. (a) Probability density function and cumulative probability density of the particle size. (b) 700HR5P800MPa ($\gamma=0.5589$, $M_s=1.2178 \times 10^6$, $p_1=38.2208$, and $p_2=6.3243$) (c) 130i5P800MPa ($\gamma=0.4190$, $M_s=1.2929 \times 10^6$, $p_1=43.5334$, and $p_2=3.3797$).

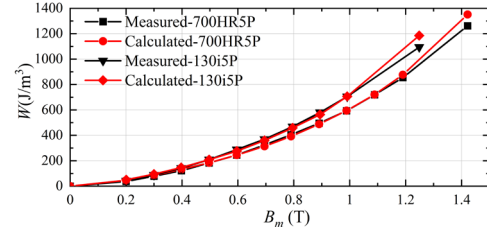


Fig. 5. Calculated and measured iron loss at 10 Hz.

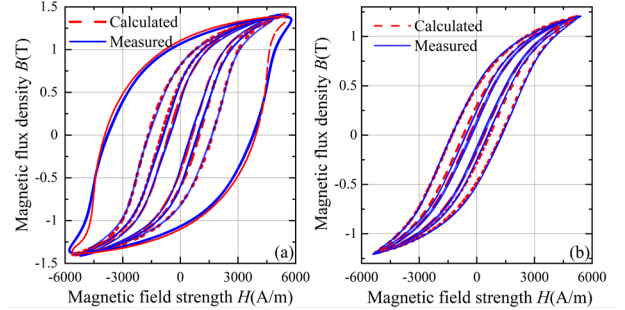


Fig. 6. Comparison between the measured and calculated hysteresis loops at 50 Hz, 100 Hz, 200 Hz and 500 Hz. (a) 700HR5P800MPa ($c=0.7691$, $\gamma=0.9221$, $M_s=1.2178 \times 10^6$, $p_1=0.0649$, $p_2=20.1223$, $p_3=0.9342$ and $p_4=0.7123$) (b) 130i5P800MPa ($c=0.8057$, $\gamma=0.6363$, $M_s=1.2929 \times 10^6$, $p_1=0.4790$, $p_2=10.4929$, $p_3=0.3267$ and $p_4=0.6721$).

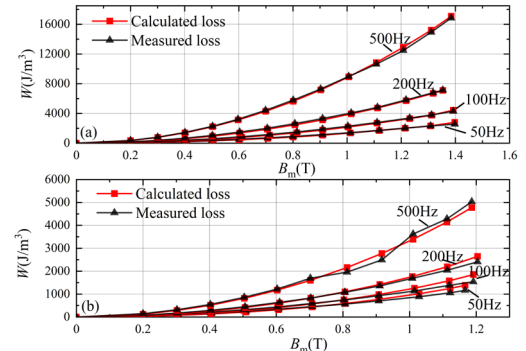


Fig. 7. Calculated and measured iron loss at different frequencies. (a) 700HR5P800MPa (b) 130i5P800MPa.

IV. CONCLUSION

This paper proposes a hysteresis model for SMCs, considering the influence of particle size distribution on magnetic properties. By integrating the advantages of the EB model and the Globus model, a comprehensive understanding of domain wall motion is obtained. Then, the static model is extended by introducing dynamic component, involving the impact of particle size on eddy current generation. By comparing with the experimental results, the validation of two types of samples leads to an overall average error below 10%. The proposed model exhibits relatively high accuracy in modelling hysteresis loops and losses across a broad range of magnetic flux densities and frequencies for SMCs with different particle sizes.

REFERENCES

- [1] P. Kolla'r, "Power loss separation in Fe-based composite materials," *J. Magn. Magn. Mater.*, vol. 327, pp. 146 – 150, Feb. 2013.
- [2] E. A. Pe'ri'go, "Past, present, and future of soft magnetic composites," *Appl. Phys. Rev.*, vol. 5, pp. 031301, Jul. 2018.
- [3] J. Liu, C. Davis, "A hysteresis model considering microstructural feature distribution," *AIP Conf. Proc.*, pp. 090018, Feb. 2016.
- [4] M. Akito, et al. "Identification of magnetization characteristics of material from measured inductance data." *IEEE Trans. Mag.*, vol. 55, no.6, pp. 1- 5, Jun. 2019.
- [5] B. Upadhaya and F. Martin, "Modelling anisotropy in non-oriented electrical steel sheet using vector jiles-atherton model," *COMPEL-Int. J. Comput. Math. Electr. Electron. Eng.*, vol. 36, no. 3, pp. 764–773, May. 2017.
- [6] R. Chen, F. Martin, Y. Li, et al. "An Energy-Based Anisotropic Vector Hysteresis Model for Rotational Electromagnetic Core Loss". *IEEE Trans. Ind Electron.*, vol.71, no.6, pp. 6084 – 6094, Jun. 2024.
- [7] M. Anhalt, "Systematic investigation of particle size dependence of magnetic properties in soft magnetic composites," *J. Magn. Magn. Mater.*, vol. 320, no. 14, pp. 366–369, Jul. 2008.
- [8] M. A. Escobar, R. Valenzuela, L. F. Magaña, "Analytical prediction of the magnetization curve and the ferromagnetic hysteresis loop," *J. Appl. Phys.*, vol. 54, pp. 1969 – 1974, Jun. 1983
- [9] C. Appino, O de La Barrière, F. Fiorillo, et al. "Classical eddy current losses in soft magnetic composites". *J. Appl. Phys.*, vol. 113, no. 17, 17A322, Mar. 2013.
- [10] M. A. Escobar, "Effect of the grain size distribution on the magnetization curve," *J. Appl. Phys.*, vol. 57, no. 6, pp. 2142–2146, Oct. 1985.
- [11] S. Yue, P. I. Anderson, Y. Li, Q. Yang, and A. Moses, "A modified inverse vector hysteresis model for nonoriented electrical steels considering anisotropy for fea," *IEEE Trans. Energy Convers.*, vol. 36, no. 4, pp. 3251–3260, Dec. 2021
- [12] G. Bertotti. Hysteresis in magnetism: for physicists, materials scientists, and engineers, vol. IX, *Gulf Professional Publishing*, 1998, pp. 255-265.
- [13] Li, Wanjia, et al. "Particles size-dependent magnetic properties of a FeSiAl soft magnetic composite with hybrid insulating coating for MHz applications." *Mater Sci Eng B*, vol. 291, pp. 116387, May.2023.
- [14] L. Zhu, J. Park, C. S Koh. "A dynamic hysteresis model based on vector-play model for iron loss calculation taking the rotating magnetic fields into account". *IEEE Trans. Mag.*, vol.54, no.3, pp. 1-4, Mar. 2018.
- [15] Pingping Guo, et al. "High-frequency losses calculating model for magnetostrictive materials considering variable DC bias." *IEEE Trans. Mag.*, vol.58, no.2, pp.1-5, May. 2021.